

A Valence Bond Description of Coordinate Covalent Bonding[†]

Alyson Ann Fiorillo and John Morrison Galbraith*

Department of Chemistry and Physics, Marist College, Poughkeepsie, New York 12601

Received: January 27, 2004; In Final Form: April 2, 2004

The coordinate covalent (dative) bonded molecules $\text{H}_3\text{N}-\text{BH}_3$, $\text{H}_3\text{N}-\text{BF}_3$, $\text{F}_3\text{N}-\text{BH}_3$, $\text{H}_3\text{N}-\text{BMe}_3$, and $\text{Me}_3\text{N}-\text{BH}_3$ have been studied using valence bond theory (VB). The classic three-structure VB picture changes slightly to account for the increased importance of the VB configuration with both electrons on the donor fragment. When the effects of geometric distortion upon molecule formation are removed, the expected trends in bond energies emerge. Addition of electron-withdrawing (F) substituents increases bond energy in $\text{H}_3\text{N}-\text{BF}_3$ and decreases bond energy in $\text{F}_3\text{N}-\text{BH}_3$. Likewise, addition of electron-donating methyl groups (Me) decreases bond energy in $\text{H}_3\text{N}-\text{BMe}_3$ and increases bond energy in $\text{Me}_3\text{N}-\text{BH}_3$. In addition, the effects of adding fluorines stepwise in the series $\text{H}_3\text{N}-\text{BH}_3$, $\text{H}_3\text{N}-\text{BH}_2\text{F}$, $\text{H}_3\text{N}-\text{BHF}_2$, $\text{H}_3\text{N}-\text{BF}_3$ has been determined. Bond energies are due to the opposing factors of electron withdrawal due to the high fluorine electronegativity and donation into the N–B bonding region by F p lone pairs. VB weights obtained by the method of Chirgwin and Coulson were unstable for coordinate covalently bonded molecules whereas no such problems were found for inverse overlap weights. VB weights in conjunction with bond energy partitioning show that the coordinate covalent bonds studied herein are predominantly charge shift bonds which owe their stability to VB structure mixing rather than any one structure alone.

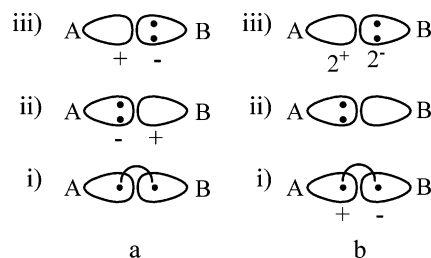
Introduction

On the basis of the familiar chemical picture of the two electron bond of Lewis¹ and Langmuir,² the conceptual strengths of valence bond theory (VB) are well known. In the classic VB picture first developed by Heitler and London,³ a bond is made up by the sharing of two electrons among separate atoms or fragments as in Scheme 1a, (i). The stabilization of this structure is derived from the mixing of the two spin determinants $A(\alpha)B(\beta)$ and $A(\beta)B(\alpha)$. This model can be refined by including ionic structures such as Scheme 1a, (ii) and (iii), which allow both electrons to be located on one fragment or the other.

The basic VB model has led to much insight into the nature of chemical bonding^{4–8} and reactivity.^{9,10} In addition to accurate bond energies, VB allows for the determination of contributions to the overall wave function from chemically relevant resonance structures as well as mixing between structures. In particular, Shaik and co-workers^{7,11} have shown that the energy of a single spin paired determinant of H_2 remains constant from bonding distances out to infinite separation thus allowing for the determination of bond energies by essentially “turning off” the bond and leaving the rest of the molecule intact.

This model is based on the idea that each fragment contributes a single electron to the two-electron bond. However, there are many examples, commonly referred to as “coordinate covalent” or “dative” type bonding, where one fragment contributes both electrons to the bond. The VB picture for coordinate covalent bonds changes slightly as shown in Scheme 1b with structure (ii) expected to contribute more to the overall wave function and be devoid of electronic charge. Although structure (iii) in Scheme 1b is expected to be very high in energy and thus contributes little to the coordinate bond, it is included herein to

SCHEME 1



be consistent with the standard three-structure VB treatment of normal covalent bonds.

The classic example of coordinate covalent bonding involves the donation of an electron pair from an amine into the vacant p orbital of a borane. The first such compound, $\text{H}_3\text{N}-\text{BF}_3$, was isolated as early as 1809 by Gay-Lussac.¹² In addition, Pearson¹³ has developed the theory of hard and soft acids and bases as a model for bonding in donor–acceptor (D–A) complexes. From that time, there have been many experimental^{14–19} and theoretical^{18–26} studies of molecules containing coordinate covalent bonds.

For example, Frenking and co-workers²² have described the bonding in this type of molecule in terms of electrostatic and covalent interactions using natural bond order (NBO)²⁷ and topological electron density analysis.²⁸ In addition, Mo and Gao²⁹ have used the block localized wave function (BLW) approach³⁰ to partition the bond energies of many donor–acceptor complexes into contributions from electrostatic, polarization, and charge-transfer terms. Both of these studies found two main groups of D–A molecules: weakly bound van der Waals complexes held together mainly by electrostatic forces and strongly bound molecules with considerable covalent and charge-transfer interactions.

As well as being theoretically significant as molecules that lie between strong *intra*- and weak *intermolecular* attractions,³¹

[†] Originally submitted for the “Fritz Schaefer Festschrift”, published as the April 15, 2004, issue of *J. Phys. Chem. A* (Vol. 108, No. 15).

* Address correspondence to this author. E-mail: John.Galbraith@Marist.edu.

TABLE 1: Transformation of Molecular Orbitals Into Ψ_{VB} for Donor–Acceptor Molecules

		D ^a	A ^b	e ^c
1	H ₃ N–BH ₃	2	2	6
2	H ₃ N–BF ₃	2	3	8
3	F ₃ N–BH ₃	3	2	8
4	Me ₃ N–BH ₃	4	2	10
5	H ₃ N–BMe ₃	2	3	8
6	H ₃ N–BH ₂ F	3	4	12
7	H ₃ N–BHF ₂	2	4	10

^a Molecular orbitals assigned to the donor fragment. ^b Molecular orbitals assigned to the acceptor fragment. ^c Number of electrons included in the VB calculation.

D–A complexes are prevalent in transition-metal chemistry, are useful in organic synthesis,^{32,33} and are thought to have beneficial physiological effects.³⁴ The present paper applies VB concepts to the coordinate covalent N–B bonds in the Lewis acid/base adducts R₃N–BR₃ where R can represent an electron-donating methyl group or an electron-withdrawing F. In doing so, the insight provided by VB in describing normal covalent bonds will be extended to coordinate donor–acceptor bonds thus complementing the existing conceptual picture of bonding in this important class of molecules.

Theoretical Methods

Computational Details. The ground-state geometries of all structures reported herein were optimized by density functional theory (DFT)^{35,36} using the B3LYP functional^{37–39} along with the 6-31G* basis set.^{40–45} Holme and Truong have shown that nonlocal exchange-correlation potentials such as B3LYP provide excellent agreement with experimental geometric parameters for these types of systems.⁴⁶ All DFT optimizations were performed with the GAUSSIAN98 suite of programs.⁴⁷

Valence bond self-consistent field (VBSCF)⁴⁸ calculations using XIAMEN99⁴⁹ were then performed on the optimized B3LYP/6-31G* geometries using the three structures in Scheme 1b. Herein, VB structures of the type *i* in Scheme 1b will be designated ϕ_{HL} in reference to the Heitler–London³ treatment of H₂ where each fragment contains one bond electron. ϕ_{C} will be used to designate the coordinate covalent bonding structure where one fragment contains both bonding electrons while neither fragment carries a charge as in Scheme 1b, ii. ϕ_{I} will be used for ionic configurations where one fragment contains both bonding electrons and both fragments carry a charge as in Scheme 1b, iii.

Construction of the VB wave functions involved preliminary restricted Hartree–Fock calculations and analysis of the resulting molecular orbitals (MOs) to determine which MOs contributed to the coordinate covalent bond. These MOs were then assigned to the donor or acceptor fragment and transformed into VB orbitals strictly localized on a particular fragment as described in Table 1. MOs not included in the orbital transformation were frozen in the VB calculation. The total wave function can then be written as in eq 1.

$$\Psi_{\text{VB}} = c_1\phi_{\text{C}} + c_2\phi_{\text{HL}} + c_3\phi_{\text{I}} \quad (1)$$

In the VBSCF procedure, the coefficients and VB orbitals are optimized simultaneously to yield the lowest possible energy. Thus, the bonding electrons are correlated while nonbonding orbitals can adjust in size and shape to the bond pair.

The VBSCF procedure can be refined by allowing a separate set of VB orbitals for each configuration. As a result, the orbitals of one configuration can “breathe” in response to the other configurations thus recovering some dynamic electron correla-

tion. This breathing orbital VB (BOVB)^{6,50} procedure yields bond energies on par with coupled cluster including single and double excitations with the perturbative addition of triple excitations [CCSD(T)].⁵ However, this procedure proved to be prohibitively expensive for the molecules studied herein. In addition, the qualitative bonding picture does not change in going from VBSCF to BOVB.^{5,11} Therefore, BOVB calculations were performed only for H₃N–BH₃ as a representative example.

Analysis of Wave Functions. The weight of each VB structure in the overall wave function was determined by both the method of Chirgwin and Coulson⁵¹ and the inverse overlap method of Gallup and co-workers.^{52,53} The Chirgwin–Coulson formulation is the VB analogue of the familiar Mulliken population analysis (eq 2).

$$w_i = c_i^2 + \sum_j c_i c_j S_{ij} \quad (2)$$

In the inverse overlap method, the unique contribution of each structure is equal to the diagonal of the reciprocal of the inverse overlap matrix, S^{-1} . The relative weights are then determined as in eq 3 and then renormalized.

$$w_i \propto \frac{|c_i|^2}{(S^{-1})_{ii}} \quad (3)$$

In this manner, a structure that contributes little by itself but a large amount through overlap will have a small weight even though the coefficient may be large.

Results and Discussion

In the following discussion, a bond energy partitioning scheme will be developed from results on the simplest coordinate covalent bond He–H⁺. H₃N–BH₃ will then be considered separately as a prototypical example of a donor–acceptor (D–A) bond. Comparisons will then be made between boramine complexes trisubstituted with F and methyl groups (Me). Last, the effect of adding fluorine substituents to the boron will be examined in detail followed by a discussion of VB weights for all species involved.

Bond Energy Partitioning. As shown by Shaik and co-workers,^{7,11} VB allows for the determination of bond energies as the difference between the three-structure VB energy and a single spin determinant referred to as the “quasiclassical” (QC) state. This technique works because of the near complete cancellation of Coulombic energy terms resulting in a nearly flat energy curve from equilibrium distances out to infinite separation. The analogous treatment for coordinate covalent bonds involves the difference between the three-structure VB energy and the coordinate covalent structure alone. As shown in Figure 1 for He–H⁺, the ϕ_{C} energy does indeed remain relatively constant from equilibrium bond distances out to infinite separation with a shallow minimum representing van der Waals interactions. Figure 1 is very similar in structure to the QC H–H curve of Shaik and co-workers.⁷

Separation of the D–A complexes herein also involves considerable geometric rearrangement among the R₃N and BR₃ fragments making a direct comparison between the $\phi_{\text{C}}/\Psi_{\text{VB}}$ energy difference and the total bond energy meaningless. A more relevant comparison would be to the difference between Ψ_{VB} and $\Psi_{\text{dist}}(\text{D} + \text{A})$ which is defined as in eq 4 where $\Psi_{\text{dist}}(\text{D})$ and $\Psi_{\text{dist}}(\text{A})$ are the wave functions of the

$$\Psi_{\text{dist}}(\text{D} + \text{A}) = \Psi_{\text{dist}}(\text{D}) + \Psi_{\text{dist}}(\text{A}) \quad (4)$$

TABLE 2: Components of VBSCF Bond Energies for Donor–Acceptor Molecules^e

		ΔE_{dist}	ΔE_C	ΔE_{CT}	$\text{BE}(\text{dist})_{\text{VB}}$	BE_{VB}	theory ^a	expt. ^a
1	H ₃ N–BH ₃	14.6	–18.1	–24.6	–42.7	–28.1	–30.7 ^b	–31.1 ^c
2	H ₃ N–BF ₃	26.4	–22.3	–30.4	–52.7	–26.3	–22.0 ^b	
3	F ₃ N–BH ₃	12.6	–5.5	–6.4	–11.9	0.7	–5.84 ^d	
4	Me ₃ N–BH ₃	18.2	–36.8	–11.9	–48.7	–30.5	–41.1 ^b	–38.3 ^c
5	H ₃ N–BMe ₃	16.3	–2.2	–30.1	–32.3	–17.4	–14.9 ^d	
6	H ₃ N–BH ₂ F	16.8	–11.1	–27.7	–38.8	–22.0		
7	H ₃ N–BHF ₂	20.7	–12.5	–28.8	–41.3	–20.6		

^a Theoretical and experimental values are reported in terms of *negative* bond dissociation energies. ^b MP2/TZ2P theoretical values of Jonas, Frenking, and Reetz (ref 22). ^c Experimental values of Haaland (ref 14). ^d HF/6-31G(d) theoretical values of Sana, Leroy, and Wilante.²⁴ ^e All energies in kcal/mol.

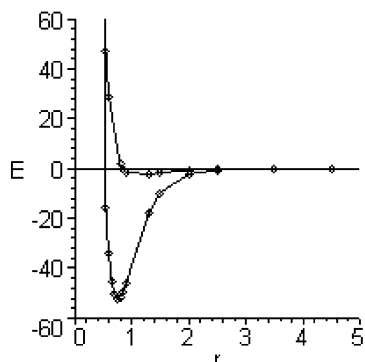


Figure 1. Potential energy surfaces for He–H⁺ stretching for the three-configuration VBSCF wave function, Ψ_{VB} , and the coordinate configuration alone, ϕ_C . Energy in kcal/mol and $r(\text{He}-\text{H}^+)$ in Å.

separated donor and acceptor with optimized geometric parameters of the donor–acceptor complex. However, the difference between ϕ_C and $\Psi_{\text{dist}}(\text{D} + \text{A})$, ΔE_C , can still be quite large (Table 2). As described by Mo and Gao,²⁹ ΔE_C is due to electrostatic and orbital polarization effects. These effects cancel out for the He–H⁺ case but not for other D–A adducts.

Thus, the total N–B bond energy can be broken down as in eq 5. Where

$$\text{BE}_{\text{VB}} = \Delta E_{\text{dist}} + \Delta E_C + \Delta E_{\text{CT}} \quad (5)$$

ΔE_{dist} is the change in energy upon distortion from the fragments at their optimized geometries to $\Psi_{\text{dist}}(\text{D} + \text{A})$, ΔE_C is the energy of ϕ_C relative to $\Psi_{\text{dist}}(\text{D} + \text{A})$, and ΔE_{CT} is the energy difference between Ψ_{VB} and ϕ_C because of inclusion of charge-transfer VB structures. ΔE_{dist} , ΔE_C , ΔE_{CT} , and BE_{VB} values for all molecules studies herein are in Table 2. Additionally, it is beneficial to consider the bond energy excluding geometric effects as in eq 6. $\text{BE}(\text{dist})_{\text{VB}}$ values are also included in Table 2.

$$\text{BE}(\text{dist})_{\text{VB}} = \Delta E_C + \Delta E_{\text{CT}} \quad (6)$$

H₃N–BH₃. When considering ϕ_C alone, H₃N–BH₃ is stabilized by 18.1 kcal/mol from the complex at infinite N–B separation (all other geometric parameters remaining constant). Upon inclusion of the ϕ_{HL} and ϕ_{I} structures, the VBSCF energy drops by 24.6 kcal/mol (29.2 kcal/mol for BOVB).⁵⁴ These values, along with the 14.6 kcal/mol energy of distortion from the optimized fragments to their respective geometries in the H₃N–BH₃ complex,⁵⁵ ΔE_{dist} , result in a total VBSCF bond energy of 28.1 kcal/mol (32.7 kcal/mol for BOVB). This is in reasonable agreement with the experimental estimate of Haaland¹⁴ (31.1 kcal/mol) and the theoretical values of Bauschlicher and Ricca²¹ (31.1 kcal/mol) and Jonas, Frenking, and Reetz²² (30.7 kcal/mol).

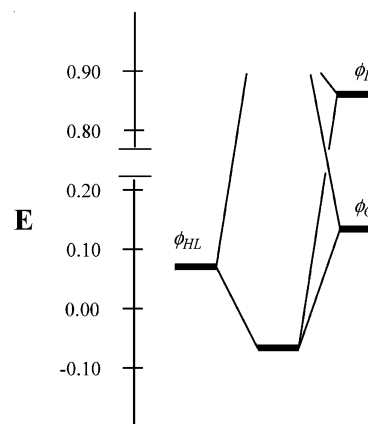


Figure 2. Three-configuration VBSCF energy mixing diagram for H₃N–BH₃. Energy in atomic units relative to $\Psi_{\text{dist}}(\text{D} + \text{A})$.

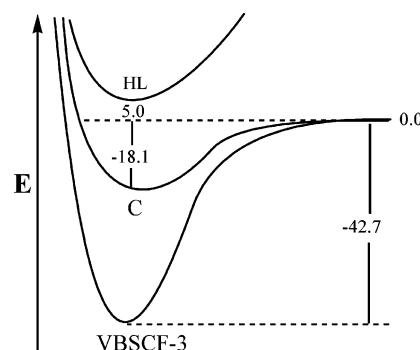


Figure 3. VBSCF potential energy surfaces for the dissociation of H₃N–BH₃. VBSCF-3 corresponds to the full three-configuration VBSCF energy. C and HL refer to the energies of Ψ_C and Ψ_{HL} (ϕ_C and ϕ_{HL} structures alone), respectively. Energies in kcal/mol relative to the NH₃ and BH₃ fragments at infinite separation with all other geometric parameters constrained to the H₃N–BH₃ values. VBSCF-3, C, and HL VB energies determined at the B3LYP/6-31G* optimized geometry.

Excluding the geometric effects in ΔE_{dist} , the VBSCF $\text{BE}(\text{dist})_{\text{VB}}$ is –42.7 kcal/mol (–47.3 kcal/mol for BOVB). ϕ_C alone only accounts for 42% of the total VBSCF $\text{BE}(\text{dist})_{\text{VB}}$ indicating that electron transfer plays an important role. Indeed, when all three structures are combined as in eq 1, ϕ_{HL} is the lowest energy configuration (most negative self-element of the Hamiltonian matrix, $H_{\text{HL,HL}}$) as seen in Figure 2. However, Figure 3 shows that in the absence of other VB structures, Ψ_{HL} (ϕ_{HL} alone) yields an energy 5.0 kcal/mol above $\Psi_{\text{dist}}(\text{D} + \text{A})$. Although the importance of ϕ_C decreases in the BOVB calculation (38%), it is clear that neither structure alone can account for the total bond energy.

The configuration weights for H₃N–BH₃ can be found in entry 1 of Table 3. Although the Chirgwin–Coulson⁵¹ and inverse overlap⁵³ weights differ in the most important config-

TABLE 3: VBSCF Weights

		ϕ_C		ϕ_{HL}		ϕ_I	
		C–C ^a	IO ^b	C–C	IO	C–C	IO
1	H ₃ N–BH ₃	0.461	0.568	0.512	0.426	0.027	0.006
2	H ₃ N–BF ₃	0.571	0.658	0.412	0.338	0.017	0.004
3	F ₃ N–BH ₃	0.319	0.335	0.551	0.558	0.130	0.107
4	Me ₃ N–BH ₃	0.477	0.594	0.512	0.406	0.011	0.001
5	H ₃ N–BMe ₃	0.577	0.723	0.429	0.277	–0.006	0.000
6	H ₃ N–BH ₂ F	2.222	0.849	–1.323	0.145	0.101	0.006
7	H ₃ N–BHF ₂	2.140	0.882	–1.184	0.117	0.043	0.001

^a Chirgwin–Coulson weights (ref 51). ^b Inverse overlap weights (ref 53).

uration at the VBSCF level,⁵⁶ it is clear that the overall wave function of H₃N–BH₃ is composed of nearly equal parts ϕ_C and ϕ_{HL} with ϕ_I making little contribution. Although previously successful^{5,11} for elucidating bonding interactions, the perturbation theory formalism for mixing VB structures^{57,58} cannot be used for H₃N–BH₃.^{59,60} However, it is apparent that the N–B bond is a result of neither ϕ_C nor ϕ_{HL} alone but primarily due to the mixing of VB structures resulting in a charge shift (CS) bonding⁴ situation.

Trisubstituted Molecules. Because of the greater electron-withdrawing capabilities of F, BF₃ should be a better Lewis acid (electron pair acceptor) than BH₃. Although the bond energy of H₃N–BH₃ is actually *greater* than H₃N–BF₃, comparison of entries **1** and **2** in Table 2 shows that this is due to the greater energetic cost of distorting the H₃N and BF₃ fragments to the H₃N–BF₃ molecular geometry. Closer examination reveals that the greater ΔE_{dist} of H₃N–BF₃ is due to the stabilization of F lone pairs by the empty B p-orbital in the planar BF₃ fragment. Neglecting geometric effects shows H₃N–BF₃ to have a more negative BE(dist)_{VB} than H₃N–BH₃ as expected. While both ΔE_D and ΔE_{CT} are greater for H₃N–BF₃ than H₃N–BH₃, ΔE_D makes up 42% of BE(dist)_{VB} in both cases.

When F replaces H on the electron donor R₃N fragment, both ΔE_C and ΔE_{CT} are smaller (entry **3** Table 2). The F atoms pull electron density from the N donor orbital thus weakening the electrostatic and polarization (ΔE_C) stabilization upon adduct formation. In addition, the fluorines hold the fragment electrons more tightly preventing transfer to the NH₃ fragment (ΔE_{CT}). However, the overall energetic contribution remains nearly the same as in H₃N–BF₃ with ΔE_C accounting for 46% of BE(dist)_{VB}.

Substituting methyl groups for hydrogens (entries **4** and **5** Table 2) results in a bond that is mostly due to ΔE_C (Me₃N–BH₃ 75% of BE(dist)_{VB}) and a bond that is mostly due to ΔE_{CT} (H₃N–BMe₃ 93% of BE(DIST)_{VB}). In addition to including the effects of charge transfer, the ϕ_{HL} and ϕ_I also serve to delocalize the bond pair and thus recover the nondynamic correlation associated with the bonding event.⁵ In Me₃N–BH₃, the methyl substituents donate electrons to the donor orbital on N thus increasing ΔE_C . However, the bond orbital is already delocalized over the methyl groups and therefore ϕ_{HL} and ϕ_I are unnecessary to relieve electron–electron repulsion. On the contrary, ϕ_{HL} and ϕ_I are needed in H₃N–BMe₃ to gain the benefits of delocalization over the methyl groups. Although the VBSCF bond energies are low in comparison to the theoretical and experimental values in Table 2, inclusion of dynamic correlation effects via the BOVB method is expected to predict values more in line with experiment.

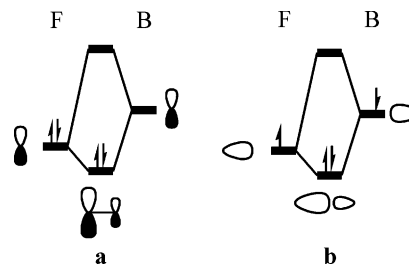
The Effect of Fluorine Substitution. In Table 2, each H attached to boron is replaced sequentially going in the order **1**, **6**, **7**, **2**. F substituents have two major effects on the N–B bond as depicted in Scheme 2. When lone pairs on F interact

TABLE 4: Mulliken Population Analysis of Fluorine Substituted Acceptor Fragments

fragment ^a	p-orbital pop. ^b	total B charge.
–BH ₃	0.013	0.092
–BH ₂ F	0.111	0.541
–BHF ₂	0.202	0.824
–BF ₃	0.264	1.202

^a Single-point calculation with fragment geometric parameters of the donor–acceptor adduct. ^b Sum of p-type basis functions in the N–B bond direction.

SCHEME 2



with the vacant p orbital on boron, the net effect is to put electron density into the bonding region (Scheme 2a) whereas the B–F σ bond serves to draw electron density away from boron because of the greater electronegativity of F (Scheme 2b). As can be seen in Table 4, there is a steady increase in the electron population of the p-orbital directed along the bond axis as the number of F substituents is increased. At the same time, the total charge of the B atom becomes more positive with increasing fluorines.

The increased positive charge on the B stabilizes the charge-transfer structures as can be seen by the ΔE_{CT} values in Table 2. However, ΔE_C initially drops in H₃N–BH₂F and then increases up through H₃N–BF₃. As described by Mo and Gao,²⁹ the stabilization of this state is due to polarization and electrostatic effects. Electrostatic stabilization is increased as the positive charge on B increases; however, stabilization due to polarization decreases as electron density increases in the boron bonding region. The interplay between these two opposing factors leads to the ΔE_C pattern seen in Table 2.

VB Weights. Determination of VB weights by the method of Chirgwin and Coulson⁵¹ (C–C) results in negative values and values greater than 1 for entries **5**, **6**, and **7** in Table 3. Indeed, there is no theoretical assurance that C–C weights will add to 1 or be positive and they are expected to give meaningful results only in simple cases.⁵² Although their significance has been discussed by Galbraith⁵ and co-workers, negative VB weights usually only appear in the least significant VB structure unlike the present case. On the other hand, weights determined by the inverse overlap (IO) method⁵³ are expected to perform better in situations where there is large configuration overlap⁵² as in the present case.

IO weights in Table 3 show that H₃N–BH₃ (entry **1**), H₃N–BF₃ (entry **2**), F₃N–BH₃ (entry **3**), and Me₃N–BH₃ (entry **4**) are made up of nearly equal parts ϕ_C and ϕ_{HL} whereas ϕ_C is the major contributor in H₃N–BMe₃ (entry **5**), H₃N–BH₂F (entry **6**), and H₃N–BHF₂ (entry **7**). In these three molecules, ϕ_C is the lowest energy structure in their respective versions of Figure 3.⁶¹ These results in conjunction with the bond energy breakdown in Table 2 indicate CS bonding.⁴ As discussed by Shaik and co-workers,^{4,5,8,11} CS bonding occurs when the major stabilizing force of the bond comes from the mixing of VB structures rather than any one structure alone as is the case in all molecules studied herein with the exception of Me₃N–BH₃.

Conclusions

The classic three-structure valence bond picture of chemical bonding changes slightly in coordinate covalent bonding with ϕ_C contributing more and ϕ_{HL} contributing less to the overall wave function. While it is possible to determine bond energies within the molecular environment for normal covalent bonds by utilizing the quasi-classical state, the analogous procedure for coordinate covalent bonds is not possible because of stabilization from electrostatics and orbital polarization.

When the total bond energy is broken down into effects from geometric distortion, ΔE_{dist} , the coordinate VB structure, ΔE_C , and charge-transfer VB structures, ΔE_{CT} , the effects of electron-withdrawing fluorine and electron-donating methyl substituents become readily apparent. When fluorines are added one at a time to the electron-accepting fragment, the total energy depends on the interplay between electron donation from F lone pairs into the bonding region of the boron and overall electron withdrawal from B because of the high electronegativity of F.

In addition, VB wave functions were analyzed in terms of weights of individual configurations. While weights obtained by the method of Chirgwin and Coulson⁵¹ produced unreasonable results, inverse overlap weights⁵³ show most of the molecules herein to be made up of nearly equal parts ϕ_C and ϕ_{HL} . In conjunction with bond energy decomposition results, VB weights show the donor–acceptor bonds studied herein to be charge shift bonds where mixing of configurations rather than any one configuration alone is responsible for the bonding event.

Acknowledgment. We thank Dr. Michael Tannenbaum for ongoing support of this and other research at Marist College. A. A. F. was partially funded by a Marist College Science Undergraduate Research Partnership. This paper is dedicated to Fritz Schaefer on the event of his 60th birthday.

References and Notes

- (1) Lewis, G. N. *J. Am. Chem. Soc.* **1916**, *38*, 762.
- (2) Langmuir, I. *J. Am. Chem. Soc.* **1919**, *41*, 868 and 1543.
- (3) Heitler, W.; London, F. *Z. Physik* **1927**, *44*, 455.
- (4) Shaik, S.; Maitre, P.; Sini, G.; Hiberty, P. C. *J. Am. Chem. Soc.* **1992**, *114*, 7861.
- (5) Galbraith, J. M.; Shurki, A.; Shaik, S. *J. Phys. Chem.* **2000**, *104*, 1262.
- (6) Hiberty, P. C.; Humbel, S.; Danovich, D.; Shaik, S. *J. Am. Chem. Soc.* **1995**, *117*, 9003.
- (7) Hiberty, P. C.; Danovich, D.; Shurki, A.; Shaik, S. *J. Am. Chem. Soc.* **1995**, *117*, 7760.
- (8) Shurki, A.; Hiberty, P. C.; Shaik, S. *J. Am. Chem. Soc.* **1999**, *121*, 822.
- (9) Shaik, S.; Wu, W.; Dong, K.; Song, L.; Hiberty, P. C. *J. Phys. Chem. A* **2001**, *105*, 8226.
- (10) Shaik, S.; Shurki, A. *Angew. Chem., Int. Ed.* **1999**, *38*, 586–625.
- (11) Galbraith, J. M.; Blank, E.; Shaik, S.; Hiberty, P. C. *Chem. Eur. J.* **2000**, *6*, 425.
- (12) Gay-Lussac, J. L.; Thénard, J. L. *Mem. Phys. Chim. Soc. Arcueil* **1809**, *2*, 210.
- (13) Pearson, R. G. *Hard and Soft Acids and Bases*; Dowden, Hutchinson and Ross: Stroudsburg, PA, 1973.
- (14) Haaland, A. *Angew. Chem., Int. Ed.* **1989**, *28*, 992.
- (15) Cassoux, P.; Kuczowski, R. L.; Bryan, P. S.; Taylor, R. C. *Inorg. Chem.* **1975**, *14*, 126.
- (16) Thorne, L. R.; Suenram, R. D.; Lovas, F. J. *J. Chem. Phys.* **1983**, *78*, 167.
- (17) Fujiang, D.; Fowler, J.; Legon, A. C. *J. Chem. Soc., Chem. Commun.* **1995**, 113.
- (18) Fiacco, D. L.; Mo, Y.; Hunt, S. W.; Ott, M. E.; Roberts, A.; Leopold, K. R. *J. Phys. Chem. A* **2000**, *105*, 484.
- (19) Kuczowski, A.; Schulz, S.; Nieger, M.; Schreiner, P. R. *Organometallics* **2002**, *21*, 1408.
- (20) Timoshkin, A. Y.; Frenking, G. *J. Am. Chem. Soc.* **2002**, *124*, 7240.
- (21) Bauschlicher, C. W.; Ricca, A. *Chem. Phys. Lett.* **1995**, *237*, 14.
- (22) Jonas, V.; Frenking, G.; Reetz, M. T. *J. Am. Chem. Soc.* **1994**, *116*, 8741.
- (23) Leroy, G.; Sana, M.; Wilante, C. *Theor. Chim. Acta* **1993**, *85*, 155.
- (24) Sana, M.; Leroy, G.; Wilante, C. *Organometallics* **1991**, *10*, 264 and **1993**, *11*, 781.
- (25) Binkley, J. S.; Thorne, L. R. *J. Chem. Phys.* **1983**, *79*, 2932.
- (26) Zirz, C.; Ahlrichs, R. *J. Chem. Phys.* **1981**, *75*, 4980.
- (27) Reed, A. E.; Curtiss, L. A.; Weinhold, F. *Chem. Rev.* **1988**, *88*, 899 and references therein.
- (28) Bader, R. W. F. *Atoms in Molecules*; Clarendon Press: Oxford, 1994.
- (29) Mo, Y.; Gao, J. *J. Phys. Chem. A* **2001**, *105*, 6530.
- (30) Mo, Y.; Gao, J.; Peyerimoff, S. D. *J. Chem. Phys.* **2000**, *112*, 5530.
- (31) Leopold, K. R.; Canagaratna, M.; Phillips, J. A. *Acc. Chem. Res.* **1997**, *30*, 57.
- (32) Reetz, M. T. *Acc. Chem. Res.* **1993**, *26*, 462.
- (33) Reetz, M. T. *Angew. Chem., Int. Ed. Engl.* **1984**, *23*, 556.
- (34) Fisher, L. S.; McNeil, K.; Butzen, J.; Holme, T. A. *J. Phys. Chem. B* **2000**, *104*, 3744.
- (35) Hohenberg, H. B.; Kohn, W. *Phys. Rev. B* **1964**, *136*, 864.
- (36) Kohn, W.; Sham, L. J. *Phys. Rev. B* **1965**, *140*, 1133.
- (37) Becke, A. D. *J. Chem. Phys.* **1993**, *98*, 5648.
- (38) Lee, C.; Yang, W.; Parr, R. G. *J. Chem. Phys.* **1988**, *37*, 785.
- (39) Miehlisch, B.; Savin, A. S. H.; Preuss, H. *Chem. Phys. Lett.* **1989**, *157*, 200.
- (40) Ditchfield, R.; Hehre, W. J.; Pople, J. A. *J. Chem. Phys.* **1971**, *54*, 724.
- (41) Hehre, W. J.; Ditchfield, R.; Pople, J. A. *J. Chem. Phys.* **1972**, *56*, 2257.
- (42) Hariharan, P. C.; Pople, J. A. *Mol. Phys.* **1974**, *27*, 209.
- (43) Hariharan, P. C.; Pople, J. A. *Theor. Chim. Acta* **1973**, *28*, 213.
- (44) Gordon, M. S. *Chem. Phys. Lett.* **1980**, *76*, 163.
- (45) Binning, R. C. J.; Curtiss, L. A. *J. Comput. Chem.* **1990**, *11*, 1206.
- (46) Holme, T. A.; Truong, T. N. *Chem. Phys. Lett.* **1993**, *215*, 53.
- (47) Frisch, M. J.; Trucks, G. W.; Schlegel, H. B.; Scuseria, G. E.; Robb, M. A.; Cheesman, J. R.; Zakrzewski, V. G.; Montgomery, J. A.; Stratmann, R. E.; Burant, J. C.; Dapprich, S.; Millam, J. M.; Daniels, A. D.; Kudin, K. N.; Strain, M. C.; Farkas, O.; Tomasi, J.; Barone, V.; Cossi, M.; Cammi, R.; Mennucci, B.; Pomelli, C.; Adamo, C.; Clifford, S.; Ochterski, J.; Petersson, G. A.; Ayala, P. Y.; Cui, Q.; Morokuma, K.; Malick, D. K.; Rabuck, A. D.; Raghavachari, K.; Foresman, J. B.; Cioslowski, J.; Ortiz, V.; Stefanov, B. B.; Liu, G.; Liashenko, A.; Piskorz, P.; Komaromi, I.; Gomperts, R.; Martin, R. L.; Fox, D. J.; Keith, T.; Al-Lahm, M. A.; Peng, C. Y.; Nanyakkara, A.; Gonzalez, C.; Challacombe, M.; Gill, P. W. M.; Johnson, B. G.; Chen, W.; Wong, M. W.; Andres, J. L.; Head-Gordon, M.; Replogle, E. S.; Pople, J. A. *Gaussian 98*, revision A.11; Gaussian, Inc.: Pittsburgh, PA, 1998.
- (48) van Lenthe, J. H.; Balint Kurti, G. G. *J. Chem. Phys.* **1983**, *78*, 5699.
- (49) Wu, W.; Song, L.; Mo, Y.; Zhang, Q. Department of Chemistry, The State Key Laboratory for Physical Chemistry of Solid Surfaces and Institute of Physical Chemistry, Xiamen, 361005, P. R. China, 1999.
- (50) Hiberty, P. C. *J. Chem. Phys.* **1994**, *101*, 5969.
- (51) Chirgwin, B. H.; Coulson, C. A. *Proc. R. Soc. London, Ser. A* **1950**, *2*, 196.
- (52) Gallup, G. *Valence Bond Methods: Theory and applications*; Cambridge University Press: New York, 2002.
- (53) Gallup, G.; Norbeck, J. M. *Chem. Phys. Lett.* **1973**, *21*, 495.
- (54) BOVB differs from VBSCF only when multiple VB configurations are involved.
- (55) This large relaxation energy (14.7 kcal/mol) is primarily due to the BH₃ fragment which is pyramidal in the H₃N–BH₃ molecule but planar by itself.
- (56) IO BOVB weights are 0.339, 0.643, and 0.018 and C–C weights are 0.307, 0.639, and 0.054 for ϕ_C , ϕ_{HL} , and ϕ_I respectively.
- (57) Shaik, S.; Hiberty, P. C. *Adv. Quantum Chem.* **1995**, *26*, 99.
- (58) Shaik, S. S. In *New Concepts for Understanding Organic Reactions*; Betrán, J., Csizmadia, I. G., Eds.; Kluwer Academic Publishers: Norwell, MA, 1989; Vol. C267.
- (59) To use perturbation theory arguments the equation, $(H_{ij} - H_{ii}S_{ij})^2 \ll |H_{ii} - H_{jj}|$, must be satisfied where i and j denote different configurations. In the present case $(H_{ij} - H_{ii}S_{ij})^2$ is actually larger than $|H_{ii} - H_{jj}|$.
- (60) Albright, T. A.; Burdett, J. K.; Whangbo, M.-H. *Orbital Interactions in Chemistry*; Wiley-Interscience: New York, 1985.
- (61) The same is true of H₃N–BF₃ where ϕ_C also has the largest weight although not significantly larger.